

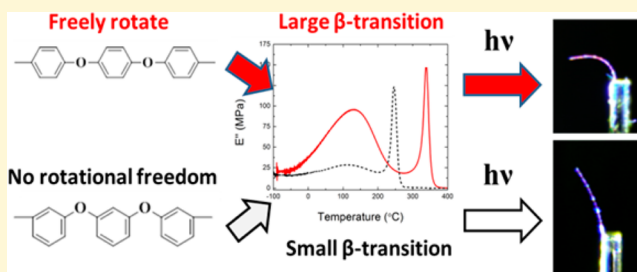
Molecular Engineering of Azobenzene-Functionalized Polyimides To Enhance Both Photomechanical Work and Motion

Jeong Jae Wie,^{†,§} David H. Wang,^{‡,§} Kyung Min Lee,[†] Loon-Seng Tan,^{*} and Timothy J. White^{*}

Materials & Manufacturing Directorate, Air Force Research Laboratory, Wright-Patterson Air Force Base, Ohio 45433-7750, United States

Supporting Information

ABSTRACT: Photomechanical effects in polymeric materials directly convert input photonic energy into a macroscopic mechanical output. The photoinitiated mechanical output of these materials is typically dominated by classical mechanics, primarily derived from the material stiffness and sample geometry. Accordingly, large magnitude shape change (e.g., motion) is typically traded for large magnitude force generation. Here, we report on the systematic preparation and comparison of photomechanical effects in a set of isomerically varied linear and cross-linked azobenzene-functionalized materials that demonstrate the critical role of segmental mobility (evident in the magnitude of the β -transition) to assimilate the typically exclusive properties of large force generation and large shape change in a single material.



INTRODUCTION

Azobenzene is perhaps the most ubiquitous photochromic moiety due to its thermal stability,¹ resolved isomeric forms,² and capacity to exhibit liquid crystallinity.³ Photoisomerization of azobenzene in glassy polymeric materials have been examined for potential utility in both optics (volume and surface relief gratings^{4–6} and nonlinear optical materials^{7–9}) and mechanics (actuators,^{10–17} sensors,^{18–22} and dynamic surfaces^{23,24}). The efficient transduction of light into mechanical (photomechanical) work in polymeric materials or composites is a complex interplay of mechanics, optics, photochemistry, polymer chemistry, and polymer physics. Prior examinations of photomechanical effects in azobenzene-functionalized polymeric materials and composites have detailed the contribution of a number of fundamental considerations such as chromophore concentration,^{25,26} geometry,^{27–29} or processing^{30–32} that confirm expected correlations to classical mechanics in which photogenerated force is traded off for displacement. In order to realize the promise of these materials as wireless energy transducers or shape-programmable actuators, materials that assimilate high performance characteristics (higher modulus, increased glass transition temperature (T_g), large magnitude shape responses, and force generation) must be developed.

A polymeric material undergoes a number of transitions in a temperature cycle. The most well known of these thermal characteristics is the glass transition temperature (T_g or T_α), wherein a polymeric material transforms from glassy to rubbery. T_α is associated with cooperative displacement of 3–5 Kuhn segments that are each composed of dozens of monomeric units.³³ Polymeric materials also exhibit a number sub- T_α transitions including the β -, γ -, and δ - transitions. Of primary

importance to the work examined here, the β -transition is associated with larger scale (whole side chains and localized groups of four to eight backbone atoms) segmental mobility of a polymer on a length scale comparable to the Kuhn segment.^{33–35} In aromatic polyimides such as the materials examined here, the β -transition usually originates from rotational mobility of benzene rings and is observed at temperatures ranging from 370 to 600 K.³⁶

Photoisomerization of azobenzene has been widely studied as a means to probe the physics of glassy polymers. As reviewed by Torkelson³⁷ and Teboul,³⁸ the sensitivity of azobenzene photochemistry to the local environment of the polymeric host has been shown to depend on the crystallinity, free volume, and molecular architecture. These factors have been shown to affect the optical performance of surface relief gratings written into azobenzene-functionalized polymers with patterned irradiation.^{39–42} In prior examinations of photomechanical effects in azobenzene-functionalized polymeric materials, the contribution of the physics of the local glassy network has been comparatively less studied.^{42,43} Recently, we have detailed the impact of crystallinity¹⁶ and physical aging (free volume)⁴⁴ on the photomechanical response of glassy, azobenzene-functionalized polyimide materials.

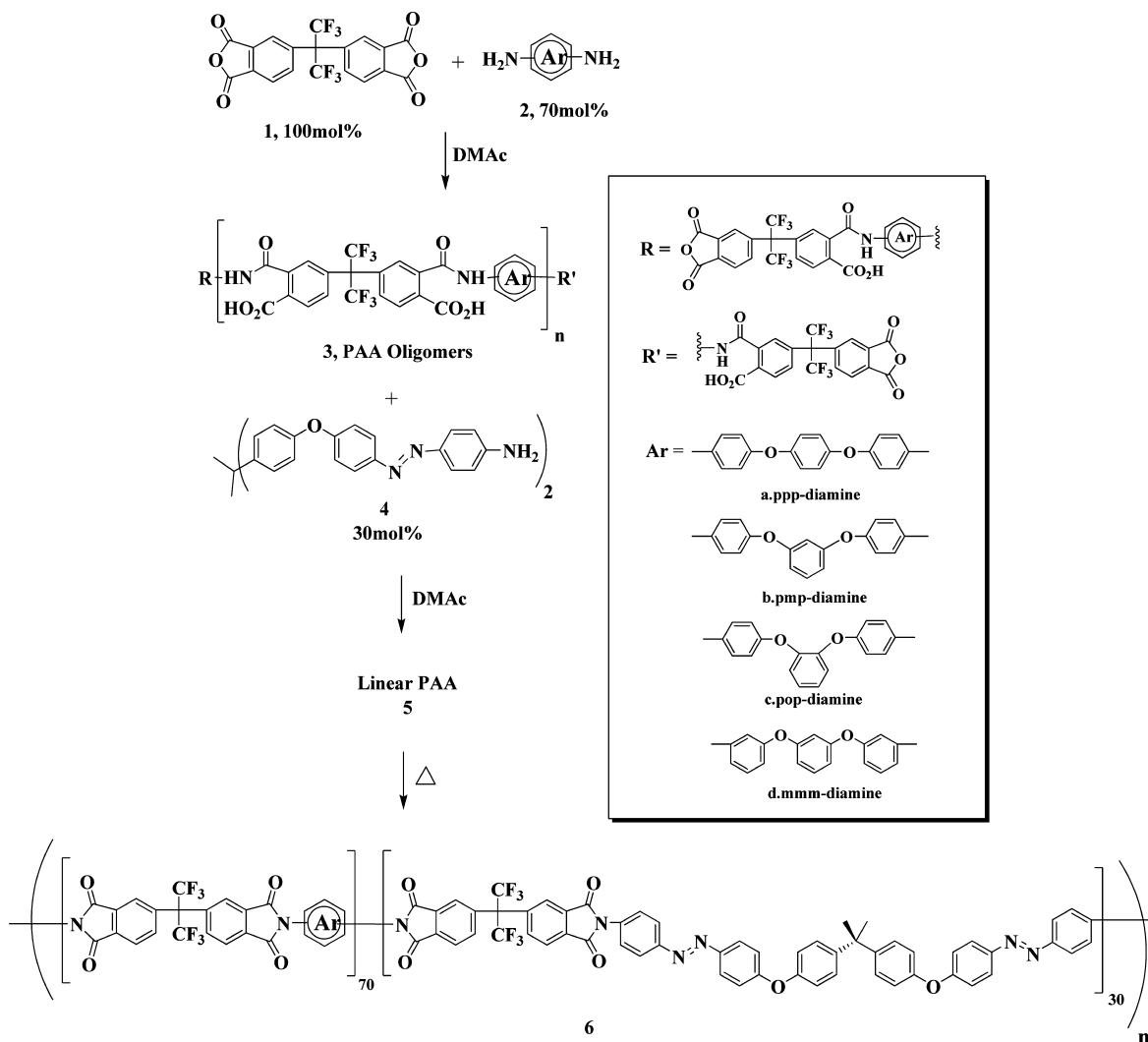
On the basis of the presumed photochemical mechanism (*trans*–*cis*–*trans* reorientation) for materials irradiated with blue–green light (in this case, 445 nm), the segmental mobility of the polymer network should be among the most critical variables in enabling the molecular-level photochemistry to be

Received: May 23, 2014

Revised: August 27, 2014

Published: August 29, 2014

Scheme 1. Synthetic Procedure for Linear Polyimides



transduced through the network to result in large scale macroscopic photomechanical responses visualized as cantilever bending or quantified via stress measurements. However, the role of segmental mobility has not been explicitly demonstrated in photomechanical experiments. The work presented here documents the synthesis of a set of isomerically varied linear and cross-linked azobenzene-functionalized polyimides that were designed to elucidate the role of segmental mobility on photomechanical effects in azobenzene-functionalized polyimide materials.

EXPERIMENTAL SECTION

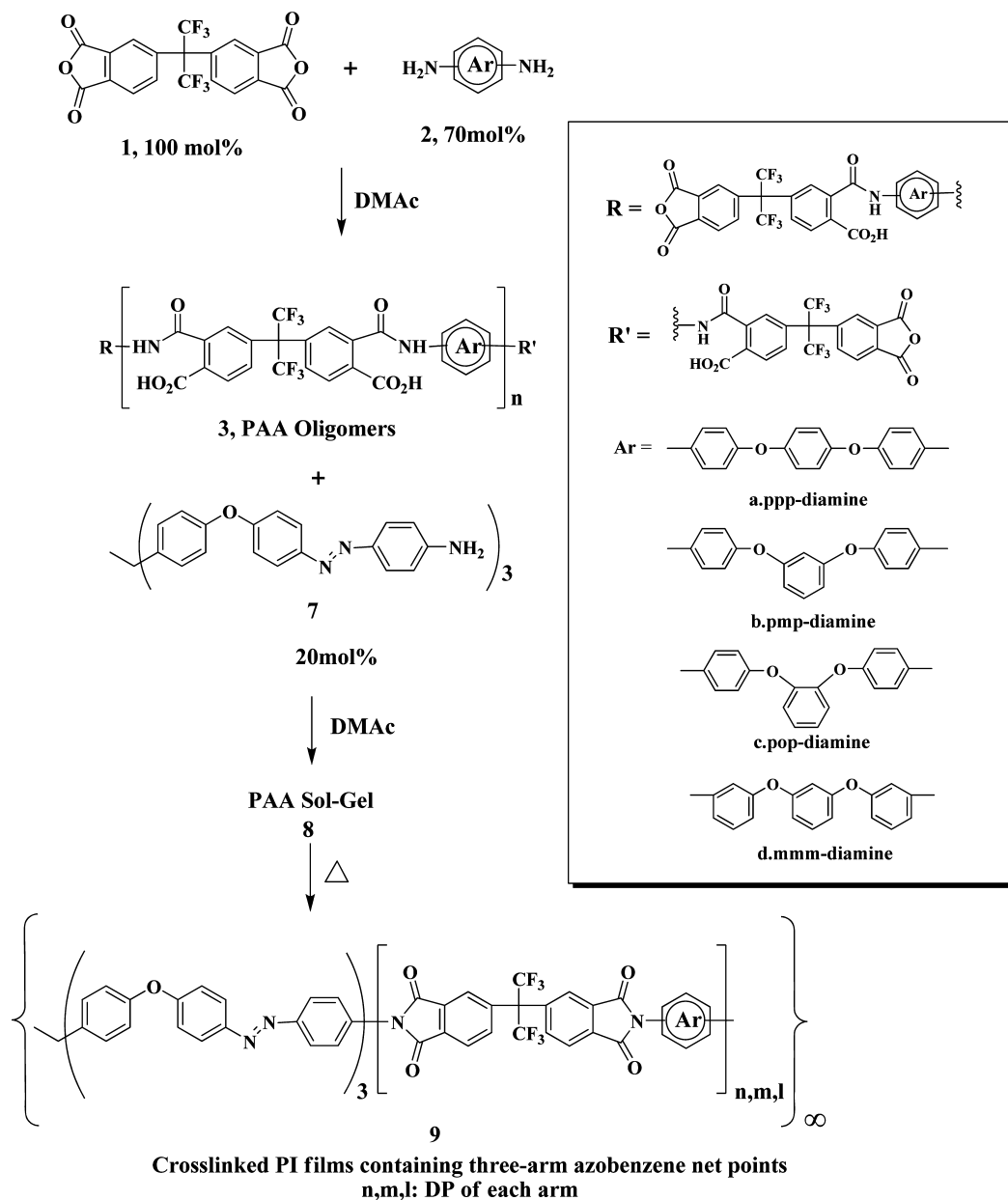
The linear and cross-linked azobenzene-functionalized polyimides are synthesized according to a two-step route, as illustrated in Schemes 1 and 2, respectively,^{35,45} and their chemical structures are shown in Figure 1. The positional isomer variants of APB diamine (mmm-, ppp-, pmp-, and pop-) were co-polymerized with 1,1,1,3,3,3-hexafluoro-2,2-bis(4-phthalic anhydride)-propane (6FDA). Briefly, 100 mol % of 6FDA and 70 mol % of an APB diamine were dissolved under a nitrogen atmosphere in *N,N*-dimethylacetamide (DMAc) at room temperature for 24 h to generate poly(amic acid) oligomers (PAA) with terminal anhydride groups. In order to maintain the same concentrations of azobenzene in both linear and cross-linked PIs, 30 mol % azobenzene diamine (4) and 20 mol % of azobenzene triamine (7) were added. The resulting PAA sol-gel precursor was poured onto

glass slides and cured in an oven, with stepwise ramping to 300 °C to fully imidize the polymer films. After preparation, the materials were subjected to near-identical cooling conditions with flowing nitrogen to limit contributions from thermal history. Accordingly, the samples examined here are not physically aged as in our prior work.⁴⁴ To facilitate the discussion that follows, the polyimide materials are ascribed with (i) L- for linear and X- for cross-linked, (ii) three-letter isomeric patterns of the APB diamine, and (iii) the diimide structure (DI) of the dianhydride (6FDA). For example, L-mmm-6FDI is linear 6FDI containing phenylene rings that are interconnected in the three meta-positions.

On the basis of previous works,^{41–43} we expect that the largest difference in segmental mobility to be observed in materials prepared with mmm- and ppp-APB. Accordingly, the main text of this work focuses on the characterization and photomechanical response of L-mmm-6FDI, L-ppp-6FDI, X-mmm-6FDI, and X-ppp-6FDI. Results collected from the analysis of the L-pmp-6FDI, L-pop-6FDI, X-pmp-6FDI, and X-pop-6FDI are included in the Supporting Information.

The materials were characterized by wide-angle X-ray scattering (WAXS), dynamic mechanical analysis (DMA), and UV–vis spectroscopy to confirm that the photomechanical response of the materials is not subject to secondary contributions from morphology or thermomechanical properties. The diffraction patterns for the eight materials examined here are presented in Figure S1 (Supporting Information). All materials (L-xxx-6FDI and X-xxx-6FDI) are completely amorphous. The thermomechanical properties and photomechanical stress of the materials were examined with a stress-

Scheme 2. Synthetic Procedure for Cross-Linked Polyimides



controlled DMA (TA Instruments, Q800, heating rate of 4 °C/min, 1 Hz frequency, nitrogen atmosphere) and strain-controlled DMA (TA Instruments, RSA3), respectively.

RESULTS AND DISCUSSION

A number of factors can influence the photomechanical response of azobenzene-functionalized polyimides including azobenzene concentration,^{26,46} chemical composition,^{29,47} crystallinity,¹⁶ and modulus.^{29,47} To avoid complications from these contributing factors, a set of linear and cross-linked azobenzene-functionalized polyimides was prepared by polymerizing four positional isomer variants of the diamine monomer with of the generic structure aminophenoxybenzene (APB), where the three-letter designations (mmm, ppp, pmp, and pop) are used to indicate the substitution patterns, namely, ortho (o or 1,2), meta (m or 1,3), and para (p or 1,4) of the first, second, and third phenylene ($-C_6H_4-$) rings. Accordingly, the azobenzene-functionalized polyimide materials examined

here are expected to maintain nearly identical azobenzene composition, crystallinity, and thermomechanical properties. Prior work has employed a similar strategy to determine the impact of segmental mobility of different positional isomers in polyimide membranes for gas separation applications.^{48–50} Similar to those results, we expect that segmental rotational motion of benzene rings will strongly depend on whether the phenylene groups in the aromatic polyimides are interconnected in the meta, ortho, or para position.⁵⁰ Notably, the large differences in rotational mobility of the meta and para isomers and the resulting influence on segmental mobility are perhaps most evident in the β -transition of the materials.⁵⁰

Table 1 summarizes the thermomechanical properties for L-mmm-6FDI, L-ppp-6FDI, X-mmm-6FDI, and X-ppp-6FDI. The materials were subjected to three heating/cooling cycles before measurement to ensure no contribution from thermal history. Both L-ppp-6FDI and X-ppp-6FDI exhibit slight increases in storage modulus, β -transition temperature (T_β),

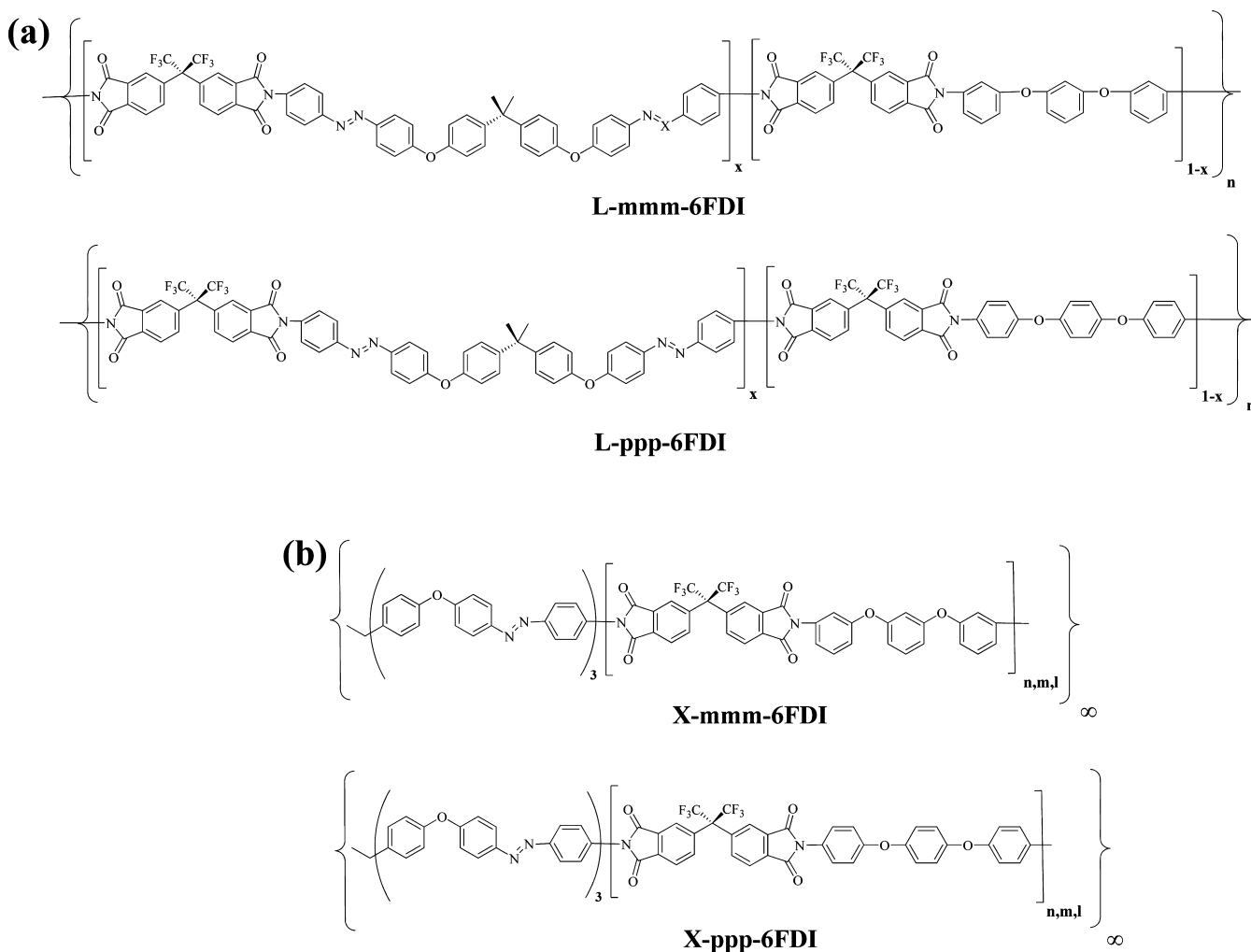


Figure 1. Chemical structures of (a) linear polyimides and (b) cross-linked polyimides.

Table 1. Summary of Thermomechanical and Absorption Properties of Linear and Cross-Linked Polyimides^a

sample code	E' (GPa)	T_{β} (K)	T_{α} (K)	T_{β}/T_{α}	$1 - (A_{350}/A_{350,0})$	dichroism
L-mmm-6FDI	2.27	382.0	520.95	0.73	0.21	1.15
L-ppp-6FDI	2.38	392.7	576.45	0.72	0.20	1.14
X-mmm-6FDI	2.40	408.4	549.05	0.74	0.15	1.09
X-ppp-6FDI	2.77	424.7	613.65	0.69	0.16	1.10

^aStorage modulus (E') is reported at 25 °C.

and glass transition temperature (T_{α}) compared to that of mmm-6FDI analogues. The ratio of the temperature of the β - and α -transitions [T_{β} (K)/ T_{α} (K)] is governed by intermolecularly correlated displacement due to the general relation of glass transition and thermal expansion as described by Boyer's rule.⁵¹ Typically, this ratio is between 0.65 and 0.8 in polyimides.⁵² T_{β} (K)/ T_{α} (K) for the materials examined here ranges from 0.69 to 0.74.

The β -transition of L-mmm-6FDI, L-ppp-6FDI, X-mmm-6FDI, and X-ppp-6FDI are reported from the loss modulus (E'') plots presented in Figure 2a (for L-mmm-6FDI and L-ppp-6FDI) and Figure 2b (for X-mmm-6FDI and X-ppp-6FDI). In Figure 2a,b, the β -transition of L-mmm-6FDI and L-ppp-6FDI as well as X-mmm-6FDI and X-ppp-6FDI is clearly observed at temperatures below the α -transition. Notably, L-ppp-6FDI and X-ppp-6FDI exhibit a larger loss modulus value at temperatures within the β -transition (Figure 2a,b). The

difference in the magnitude of the loss modulus between the mmm and ppp isomeric forms is a strong confirmation of the positional isomer effect previously observed in polyimide membranes.^{48–50} The β -transition measured from L-mmm-6FDI and X-mmm-6FDI is likely associated with the phenyl-ether groups adjoined to the azobenzenes. As is apparent in Figure 2b, the β -transition is more pronounced in the cross-linked series. Since the numbers of para-phenylene rings responsible for this transition are the same in both the set of linear and cross-linked materials, we attribute this enhancement to a more effective stress transfer through covalently bonded cross-linked points. As is evident in Figure 2a,b and the Supporting Information, the loss modulus data for the ppp, pmp, and pop isomeric forms of L-xxx-6FDI and X-xxx-6FDI are very similar, indicating that the connectivity of the middle phenylene group may not strongly differentiate the segmental

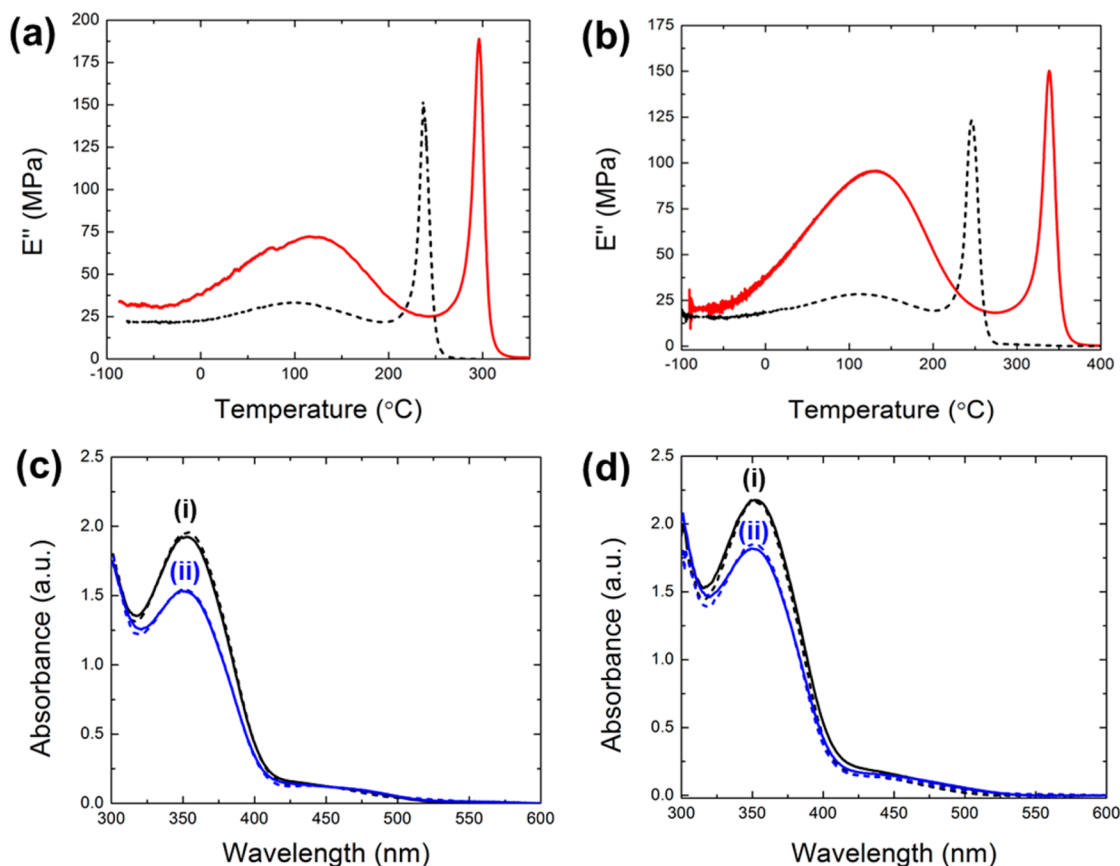


Figure 2. Temperature resolved loss modulus measurements for (a) linear and (b) cross-linked polyimides. The samples were prepared with the following gauge dimensions: 6 mm (L) \times 3 mm (W) \times 20 μm (T). Black dashed lines and red solid lines indicate 6FDI composed with mmm and ppp isomers, respectively. Absorption behaviors of spin-coated (c) linear and (d) cross-linked polyimides are obtained by UV-vis spectroscopy: (i) before light exposure or (ii) after exposure to 120 mW/cm² linearly polarized 445 nm light ($E||x$) for 1 h. Dashed lines and solid lines indicate mmm and ppp isomers, respectively.

mobility of the ppp, pmp, and pop isomeric forms of the polymers.

Photomechanical effects can be strongly biased by differences in the optical penetration of light into the film. As is evident in Figure 2c,d, both L-mmm-6FDI and L-ppp-6FDI and X-mmm-6FDI and X-ppp-6FDI have nearly identical absorption spectra before and after irradiation with 120 mW/cm² of 445 nm light. This is expected, as the materials are nearly of identical chemical composition and maintain equivalent azobenzene chromophore concentrations. The absorbance change at 350 nm as well as the dichroism of the materials after irradiation with 445 nm light are summarized in Table 1. Once again, both L-mmm-6FDI and L-ppp-6FDI and X-mmm-6FDI and X-ppp-6FDI exhibit nearly identical photochemical responses as measured by these values. Accordingly, in subsequent photomechanical characterization, it can be concluded that any differences in the response of the materials to actinic light irradiation is not attributable to the magnitude or the extent of the photochemistry that is occurring at the molecular level.

The photomechanical response of the set of linear and cross-linked azobenzene-functionalized polyimide materials was examined both by stress and cantilever bending measurements. For photogenerated stress measurements, the polyimide film was placed in DMA with minimum tension. Thereafter, stress was measured under continuous irradiation to account for slight contributions in thermal expansion and the photostationary state concentration of cis isomers. As is evident in Figure 3a,b,

the films (6 \times 3 \times 0.02 mm) impart negligible stress when subjected to light polarized 45 $^{\circ}$ to the long axis of the cantilever (E45x). Adjusting the orientation of the light polarization such that the electric field vector of the polarized 445 nm light is parallel to the gauge length ($E||x$) generates positive stress, which is monitored over time. Comparatively, larger photo-generated stress is measured from higher modulus L-ppp-6FDI and X-ppp-6FDI materials compared to that from the L-mmm-6FDI and X-mmm-6FDI polyimides. Thus, the photogenerated stress measured in the azobenzene-functionalized polyimides is strongly dependent on the modulus of the material, as expected from classical mechanics.

The temporal response of the materials both during and after irradiation was examined in cantilevers (6 \times 0.1 \times 0.02 mm) that were irradiated with linearly polarized (parallel to long axis of the cantilever, $E||x$) 445 nm light at 120 mW/cm² for 1 h. Thermal imaging during irradiation has been used to confirm that this light intensity does not cause macroscopic temperature increase ($<3^{\circ}\text{C}$) for polymeric materials containing a similar concentration of azobenzene chromophores.⁵³ The magnitude of the photoinduced deflection of cantilevers composed from linear azobenzene-functionalized polyimides (Figure 3c) is less than that observed in cross-linked azobenzene-functionalized polyimides of a similar chemical makeup. Within the set of either linear or cross-linked polyimide materials, the connectivity of the phenylene rings strongly influences the resulting response. As is evident in Figure 3c,d, larger photomechanical

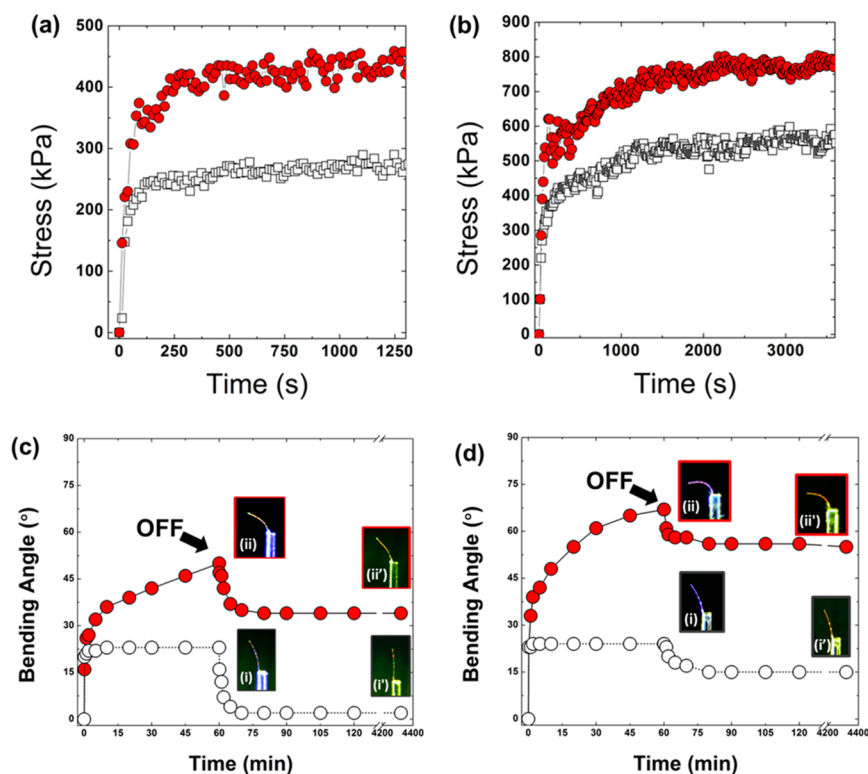


Figure 3. Time-resolved photogenerated stress and bending angle measurement for meta (○) and para (red circle) isomers in (a, c) linear and (b, d) cross-linked polyimides. Photogenerated stress of polyimides is measured upon exposure to 60 mW/cm² of 445 nm light ($E||x$). Before the measurement, polyimides are pre-exposed to E45x light. The sample dimensions were 6 mm (L) × 3 mm (W) × 20 μm (T). Bending measurement was conducted on films of the same dimensions: 6 mm (L) × 0.1 mm (W) × 20 μm (T). The films were subjected to 445 nm light ($E||x$) at 120 mW/cm² intensity for 1 h and subsequently relaxed in dark. For both (c) and (d), images are labeled (i) and (ii) to denote 6FDI composed of (i) meta (○) and (ii) para (red circle) isomers. Images marked with (') are taken after 3 days dark relaxation.

bending was observed in L-ppp-6FDI (50°) and X-ppp-6FDI (67°) than in L-mmm-6FDI (23°) or X-mmm-6FDI (24°). The photomechanical response of the ppp (Figure 3a–d), pmp (Supporting Information), and pop (Supporting Information) forms of L-xxx-6FDI and X-xxx-6FDI are not significantly different, indirectly confirming the correlation among loss modulus, segmental mobility, and photomechanical responses observed here. Notably, there are also differences in the shape retention after the cantilevers were stored in the dark for 3 days, wherein L-ppp-6FDI retains 68% of the deflection, L-mmm-6FDI retains only 9% of the deflection, X-ppp-6FDI retains 82% of the deflection, and X-mmm-6FDI retains 62% of the deflection. Our prior studies have examined shape retention in both azobenzene-functionalized liquid crystal networks and polyimides. As discussed in those reports, the irradiation employed is not sufficiently large to induce macroscopic heating of the material above T_g of these polyimides (248–297 °C), and we do not believe the shape retention is due to thermal fixing. As in our previous examination,⁴⁴ we attribute the shape retention to local distortion of the polymer network caused by the photochemical mechanisms that are primarily subject to the viscoelastic properties of the glassy polymer network.

Typically, the photomechanical response of azobenzene-functionalized polyimides is dictated by the modulus (stiffness) of the material. Accordingly, actinic irradiation of high-modulus (stiffness) materials exhibits lower magnitude deflections and larger magnitude stress (force) than that of lower-modulus (stiffness) materials. As discussed above, designing azobenzene-

functionalized polyimide materials at the molecular level to enhance segmental mobility breaks this expected trend in that L-ppp-6FDI and X-ppp-6FDI exhibit larger stress generation (force) and larger deflection (motion) than that of L-mmm-6FDI and X-mmm-6FDI. It should be noted, however, that photomechanical experiments at 100 °C potentially indicate a complex interplay among enhanced segmental mobility and dissipation of the photogenerated effects. Accordingly, the room temperature experiments reported in this study may be at an optimal temperature regime to distinguish the contribution of segmental mobility to the enhancement of the photomechanical responses measured here.

CONCLUSIONS

In this work, the photomechanical response of a series of linear and cross-linked azobenzene-functionalized polyimides is examined to explore the contribution of segmental mobility on the photogenerated force and displacement. Polyimides prepared with para connectivity (ppp) maintain a higher loss modulus value at the β -transition than that of polyimides prepared with meta connectivity (mmm), which can be attributed to enhanced segmental mobility stemming from the rotational freedom of the phenylene rings. Accordingly, the enhanced segmental motion in linear and cross-linked polyimides prepared from ppp-aminophenoxybenzene (APB) results in a significantly larger magnitude of photomechanical deformation in photogenerated stress and displacement measurements. The critical role of segmental mobility is evident in comparable photomechanical responses from

polyimides prepared with pop and pmp isomeric forms that exhibit similar magnitude β transitions (data included in Supporting Information). Typically, the enhancement of photogenerated stress is accompanied by a reduction in displacement. Through molecular engineering, azobenzene-functionalized polyimide materials with larger segmental mobility can assimilate large force generation and large displacement. Future examinations of azobenzene-functionalized polyimides should thus seek to employ materials chemistries that exhibit enhanced segmental mobility.

■ ASSOCIATED CONTENT

Supporting Information

Synthetic procedures, X-ray, thermomechanical, photomechanical data are provided for two other isomers (pmp and pop). This material is available free of charge via the Internet at <http://pubs.acs.org>.

■ AUTHOR INFORMATION

Corresponding Authors

*(L.-S.T.) E-mail: Loon.Tan@us.af.mil.

*(T.J.W.) E-mail: Timothy.White.24@us.af.mil.

Present Addresses

[†]J.J.W. and K.M.L. are also with Azimuth Corp., Dayton, Ohio, United States.

[‡]D.H.W. is also with UES Inc., Beavercreek, Ohio, United States.

Author Contributions

[§]J.J.W. and D.H.W. contributed equally to this work.

Notes

The authors declare no competing financial interest.

■ ACKNOWLEDGMENTS

This work was completed at Air Force Research Laboratory (AFRL) at the Wright-Patterson Air Force Base with funding from Materials and Manufacturing Directorate as well as Air Force Office of Scientific Research.

■ ABBREVIATIONS

T_g (or T_g), glass transition temperature; T_β , β -transition temperature; APB, amine-phenoxy-phenoxy-phenylene-amine; 6FDA, 1,1,1,3,3,3-hexafluoro-2,2-bis(4-phthalic anhydride)-propane; DMAc, *N,N*-dimethylacetamide; PAA, poly(amic acid); WAXS, wide-angle X-ray scattering; DMA, dynamic mechanical analysis

■ REFERENCES

- (1) Barton, D.; Hodgett, M.; Skirving, P.; Whelton, M.; Winter, K.; Vardy, C. *Can. J. Chem.* **1983**, *61*, 1712–1718.
- (2) Anderle, K.; Birenheide, R.; Werner, M. J. A.; Wendorff, J. H. *Liq. Cryst.* **1991**, *9*, 691–699.
- (3) Wu, Y. L.; Zhang, Q. J.; Kanazawa, A.; Shiono, T.; Ikeda, T.; Nagase, Y. *Macromolecules* **1999**, *32*, 3951–3956.
- (4) Ahmed, R.; Priimagi, A.; Faul, C. F. J.; Manners, I. *Adv. Mater.* **2012**, *24*, 926–931.
- (5) Vapaavuori, J.; Priimagi, A.; Kaivola, M. *J. Mater. Chem.* **2010**, *20*, 5260–5264.
- (6) Audorff, H.; Walker, R.; Kador, L.; Schmidt, H.-W. *J. Phys. Chem. B* **2009**, *113*, 3379–3384.
- (7) Yesodha, S. K.; Sadashiva Pillai, C. K.; Tsutsumi, N. *Prog. Polym. Sci.* **2004**, *29*, 45–74.
- (8) Wang, P.; Ming, H.; Zhang, J.-Y.; Liang, Z.-C.; Lu, Y.-H.; Zhang, Q.-J.; Xie, J.-P.; Tian, Y.-P. *Opt. Commun.* **2002**, *203*, 159–162.
- (9) Krupka, O. *Nonlinear Opt., Quantum Opt.* **2013**, *45*, 203–212.
- (10) Yu, Y. L.; Nakano, M.; Ikeda, T. *Nature* **2003**, *425*, 145.
- (11) Harris, K. D.; Cuypers, R.; Scheibe, P.; van Oosten, C. L.; Bastiaansen, C. W. M.; Lub, J.; Broer, D. J. *J. Mater. Chem.* **2005**, *15*, 5043–5048.
- (12) Wu, W.; Yao, L. M.; Yang, T. S.; Yin, R. Y.; Li, F. Y.; Yu, Y. L. *J. Am. Chem. Soc.* **2011**, *133*, 15810–15813.
- (13) Sun, X.; Wang, W.; Qiu, L.; Guo, W.; Yu, Y.; Peng, H. *Angew. Chem., Int. Ed.* **2012**, *51*, 8520–8524.
- (14) Jiang, Z.; Xu, M.; Li, F.; Yu, Y. *J. Am. Chem. Soc.* **2013**, *135*, 16446–16453.
- (15) White, T. J.; Tabiryan, N. V.; Serak, S. V.; Hrozhyk, U. A.; Tondiglia, V. P.; Koerner, H.; Vaia, R. A.; Bunning, T. J. *Soft Matter* **2008**, *4*, 1796–1798.
- (16) Lee, K. M.; Wang, D. H.; Koerner, H.; Vaia, R. A.; Tan, L. S.; White, T. J. *Angew. Chem., Int. Ed.* **2012**, *51*, 4117–4121.
- (17) van Oosten, C. L.; Bastiaansen, C. W. M.; Broer, D. J. *Nat. Mater.* **2009**, *8*, 677–682.
- (18) Ugur, G.; Chang, J. Y.; Xiang, S. H.; Lin, L. W.; Lu, J. *Adv. Mater.* **2012**, *24*, 2685–2690.
- (19) Loomis, J.; Panchapakesan, B. *Nanotechnology* **2012**, *23*, 215501.
- (20) Kim, H. K.; Shin, W.; Ahn, T. J. *IEEE Photonics Technol. Lett.* **2010**, *22*, 1404–1406.
- (21) Datskos, P. G.; Sepaniak, M. J.; Tipple, C. A.; Lavrik, N. *Sensors Actuators, B* **2001**, *76*, 393–402.
- (22) Pieroni, O.; Fissi, A.; Angelini, N.; Lenci, F. *Acc. Chem. Res.* **2001**, *34*, 9–17.
- (23) Liu, D.; Bastiaansen, C. W. M.; den Toonder, J. M. J.; Broer, D. J. *Angew. Chem., Int. Ed.* **2012**, *51*, 892–896.
- (24) Liu, D.; Bastiaansen, C. W. M.; den Toonder, J. M. J.; Broer, D. J. *Macromolecules* **2012**, *45*, 8005–8012.
- (25) Kondo, M.; Sugimoto, M.; Yamada, M.; Naka, Y.; Mamiya, J.-i.; Kinoshita, M.; Shishido, A.; Yu, Y.; Ikeda, T. *J. Mater. Chem.* **2010**, *20*, 117–122.
- (26) Wang, D. H.; Lee, K. M.; Yu, Z. N.; Koerner, H.; Vaia, R. A.; White, T. J.; Tan, L. S. *Macromolecules* **2011**, *44*, 3840–3846.
- (27) Corbett, D.; Warner, M. *Liq. Cryst.* **2009**, *36*, 1263–1280.
- (28) van Oosten, C. L.; Corbett, D.; Davies, D.; Warner, M.; Bastiaansen, C. W. M.; Broer, D. J. *Macromolecules* **2008**, *41*, 8592–8596.
- (29) Wang, D. H.; Lee, K. M.; Koerner, H.; Yu, Z. N.; Vaia, R. A.; White, T. J.; Tan, L. S. *Macromol. Mater. Eng.* **2012**, *297*, 1167–1174.
- (30) van Oosten, C. L.; Harris, K. D.; Bastiaansen, C. W. M.; Broer, D. J. *Eur. Phys. J. E: Soft Matter Biol. Phys.* **2007**, *23*, 329–336.
- (31) Wie, J. J.; Lee, K. M.; Smith, M. L.; Vaia, R. A.; White, T. J. *Soft Matter* **2013**, *9*, 9303–9310.
- (32) Lee, K. M.; Wang, D. H.; Koerner, H.; Vaia, R. A.; Tan, L. S.; White, T. J. *Macromol. Chem. Phys.* **2013**, *214*, 1189–1194.
- (33) Bershtein, V. A.; Egorov, V. M.; Podolsky, A. F.; Stepanov, V. A. *J. Polym. Sci., Polym. Lett. Ed.* **1985**, *23*, 371–377.
- (34) Bershtein, V. A.; Rydjov, V. A. *Dokl. ANSSSR* **1985**, *284*, 890–895.
- (35) Menard, K. P. *Dynamic Mechanical Analysis: A Practical Introduction*, 2 ed.; CRC Press: Boca Raton, FL, 2008.
- (36) Bessonov, M. I.; Koton, M. M.; Kudryavtsev, V. V.; Laius, A. A. *Polyimides, A Class of Thermostable Polymers*; Nauka: Leningrad, 1983.
- (37) Victor, J. G.; Torkelson, J. M. *Macromolecules* **1987**, *20*, 2241–2250.
- (38) Teboul, V.; Accary, J. B.; Chrysos, M. *Phys. Rev. E* **2013**, *87*, 032309.
- (39) Viswanathan, N. K.; Kim, D. Y.; Bian, S. P.; Williams, J.; Liu, W.; Li, L.; Samuelson, L.; Kumar, J.; Tripathy, S. K. *J. Mater. Chem.* **1999**, *9*, 1941–1955.
- (40) Barrett, C. J.; Natansohn, A. L.; Rochon, P. L. *J. Phys. Chem.* **1996**, *100*, 8836–8842.
- (41) Barrett, C. J.; Rochon, P. L.; Natansohn, A. L. *J. Chem. Phys.* **1998**, *109*, 1505–1516.
- (42) Toshchevikov, V.; Saphiannikova, M.; Heinrich, G. *J. Phys. Chem. B* **2011**, *116*, 913–924.

- (43) Toshchevikov, V. P.; Saphiannikova, M.; Heinrich, G. *Macromol. Symp.* **2012**, *316*, 10–16.
- (44) Lee, K. M.; Koerner, H.; Wang, D. H.; Tan, L. S.; White, T. J.; Vaia, R. A. *Macromolecules* **2012**, *45*, 7527–7534.
- (45) Wang, D. H.; Lee, K. M.; Yu, Z.; Koerner, H.; Vaia, R. A.; White, T. J.; Tan, L.-S. *Macromolecules* **2011**, *44*, 3840–3846.
- (46) Toshchevikov, V. P.; Saphiannikova, M.; Heinrich, G. *J. Chem. Phys.* **2012**, *137*, 024903.
- (47) Wang, D. H.; Wie, J. J.; Lee, K. M.; White, T. J.; Tan, L.-S. *Macromolecules* **2014**, *47*, 659–667.
- (48) Stern, S. A.; Mi, Y.; Yamamoto, H.; Stclair, A. K. *J. Polym. Sci., Part B: Polym. Phys.* **1989**, *27*, 1887–1909.
- (49) Coleman, M. R.; Koros, W. J. *J. Membr. Sci.* **1990**, *50*, 285–297.
- (50) Mi, Y.; Stern, S. A.; Trohalaki, S. J. *J. Membr. Sci.* **1993**, *77*, 41–48.
- (51) Simha, R.; Boyer, R. F. *J. Chem. Phys.* **1962**, *37*, 1003–1007.
- (52) Gillham, J. K.; Gillham, H. C. *Polym. Eng. Sci.* **1973**, *13*, 447–454.
- (53) Lee, K. M.; White, T. J. *Macromolecules* **2012**, *45*, 7163–7170.